DETECTION OF A SINGLE ROLLING ELEMENT BEARINGS FAULT VIA RELATIVE SHAFT DISPLACEMENT MEASUREMENT

Leo Sing Lim and Mohammad Shahril Osman

Department of Mechanical and Manufacturing Systems, Faculty of Engineering, Unversiti Malaysia Sarawak, 94300 Kota Samarahan, Sarawak

ABSTRACT

This paper describes with the investigation of using relative shaft displacement approach to detect early rolling element bearings fault. Rolling element bearings are among the most common elements used in the operation of rotating machines. However, they are one of the weak points in these machines where the majority of problems associated are caused by bearings failures. As a result, condition monitoring of the rolling element bearings is important in order to keep these machineries in their proper operating condition. Analysis and maintenance of any rolling element bearings failures are made much easier if any fault can be identified during its early stage. Thus, it is the aim of this research to investigate the relative shaft displacement technique for the early fault detection in rolling element bearings. Experiments were conducted on a rotor kit that simulates the actual behaviour of rotating machines. In order to simulate the early signs of fault developing, a single localized fault was induced on the outer race and the inner race for ball bearings and roller bearings, as well as on a rolling element of a roller bearing. Experimental data from the relative shaft displacement measurements due to dynamic vibrations of the shaft were analysed using time waveform analysis to detect the sudden changes in amplitude as a function of time. The experimental results show that fault signal is clearly present with positive or negative spikes, or both in the time waveform analysis depending on the type of fault that occurs and its location relative to the probe tip. Conversely, non-defective rolling element bearings exhibit a smooth time waveform curve.

Keywords : *Rolling elements bearings; Relative shaft displacement; Bearing faults*

INTRODUCTION

In recent years, rolling element bearings have spread throughout the industry as the most widely used element for transmitting forces between rotating machine components [1]. They can be found in motors, gas turbines, pumps, and in many other rotating machines. In principle, bearings can fit into two main categories; namely, fluid film bearings and rolling element bearings [2]. Fluid film bearings are the most widely used plain bearing. They rely on lubricant viscosity to separate the bearing surfaces. As metallurgy and machining techniques progressed, the rolling element bearings gained greater usage. Rolling element bearings are the most widely used of all bearing types and usually the first choice for general applications [3]. It falls into two main classifications; they are ball bearings and roller bearings. Ball bearings are classified according to its ring configurations, such as deep groove, angular contact and thrust types. Roller bearings on the other hand are classified according to the shape of the rollers, such as cylindrical, needle, taper and spherical.

Rolling element bearings failure is one of the common causes of breakdowns in most rotating machines [4; 5]. Although modern rolling element bearings are very precisely machined, they do have micro-defects that are potential sites for future damage. Improper installation practices can also reduce bearing life due to the precise tolerances. Typically, rolling element bearings have three components that can sustain damage; these components are the outer ring, inner ring and the rolling element. The signature produced by the rolling element bearings fault varies according to the particular damaged component [6].

In Roach [7], proximity probe can be used to measure shaft displacement. This probe is a non-contacting device, which directly measures rotating shaft position relative to the probe tip. Therefore, the change in position of a shaft provides a direct indication of vibration, which may be caused by the bearing faults. However, there is currently lack of research and literature on the application of proximity probe for the detection of specific rolling element bearings fault. It is hoped that with the experimental setup, it is possible to categorise and to identify different rolling element bearing faults using proximity probe.

ROLLING ELEMENT BEARINGS ANALYSIS

Bearing locations are good places to obtain an early warning of impending failure and it is important to understand the mechanism of bearing vibrations [8]. A comprehensive model for the nature of vibrations induced by a single point fault in a rolling element bearing has been proposed by McFadden and Smith [9]. Su and Lin [10] have extended the vibration model proposed by McFadden and Smith [9] to describe the bearing vibration caused by a single rolling element bearing fault and they also gave a detailed insight into the analysis of vibration spectra. Bo *et al.* [11] have presented the use of bearing vibration frequency features and time-domain characteristics for rolling element-bearing diagnosis using neural network.

An analytical model for predicting the vibration frequencies of rolling element bearings and the amplitudes of significant frequency components due to a localized defect were proposed by Tandon and Choudhury [12]. Antoniadis and Glossiotis [1] have proposed an alternative framework for analyzing rolling element bearings vibration signals based on cyclostationary analysis. Meanwhile, Ohta and Sugimoto [13] have carried out an investigation to explain the vibrations of tapered roller bearings. Gluzman [14] has illustrated some ways of recognizing an impending bearing failure, assessing its severity and correlating actual physical damage with the vibration pattern by utilizing just a conventional vibration spectrum. On the other hand, Yaziei *et al.* [15] have reported of an adaptive, statistical time frequency method for detection of bearing faults. However, the detection procedure reported by them required an extensive training for feature extraction.

Bently [16] and Bosmans [17] tested REBAM (Rolling Element Bearing Activity Monitor) transducer to diagnose rolling element bearings in their research. The research done by Bently *et al.* [18] showed that the inner race, outer race and rolling element faults can be detected by directly measuring the outer race deflection with REBAM© transducers. Unfortunately, the limitation of this approach is that when a rolling element rolls over the location of the mounting hole for the transducer, the outer race will experience a localized deformation at that area. Consequently, the transducer will pick up this deformation as a displacement signal every time a roller passes by. Therefore, the outer race fault frequency is present in the spectrum regardless whether the bearing fault exists or not.

PROPERTIES OF THE TEST BEARINGS

In this research, ball and roller bearings were used for the analysis of raceways and rolling element faults. The test bearings were the type consisting of a single row deep groove ball bearings (SKF 6204/C3) and a single row cylindrical roller bearings (Koyo NU204C3 and Koyo N204), as shown in Figure 1.

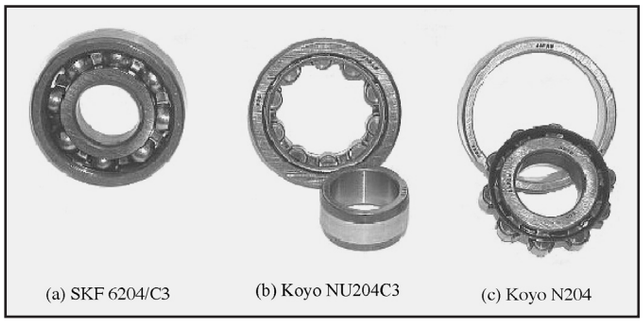

Figure 1: Test bearings

Components of the SKF 6204/C3 bearings are un-separable, whereas Koyo NU204C3 bearings inner ring and Koyo N204 bearings outer ring are completely separable. Both ball and roller bearings outer ring diameters are 47.0 mm and the inner ring diameters are 20.0 mm. A fault was carefully introduced onto the outer and inner raceways of both types of bearings by using conventional welding method. A small diameter wire was used as an electrode to create a "bump" on the raceways. In addition, a fault was also made on a roller surface of Koyo N204 bearing in order to analyse the rolling element fault, since the roller bearings are separable. The dimensions of the ball bearings (SKF 6204/C3) and roller bearings (Koyo NU204C3 and Koyo N204) are as stated in Table 1.

Table 1: Ball and roller bearings dimensions

	Ball Bearing	Roller Bearing
Number of balls or rollers, N	8	10
Bearing pitch diameter, P_d	33.5 mm	33.5 mm
Ball or roller diameter, B_d	7.9 mm	6.5 mm
Contact angle, β	0°	0°

All rolling element bearings have three frequencies corresponding to each bearing component [9]. These frequencies are called ball-pass frequency outer race (BPFO), ball-pass frequency inner race (BPFI) and ball-spin frequency (BSF). They can be derived from the bearing geometry by assuming that there is no slippage or dimensional change with load [8; 20]. For the case of the outer race fixed, the BPFO, BPFI and BSF can be calculated from the equations shown below.

$$BPFO\ (Hz) = \frac{N}{2} \times \frac{RPM}{60} \times \left(1 - \frac{B_d}{P_d}\cos\beta\right) \quad (1)$$

$$BPFI\ (Hz) = \frac{N}{2} \times \frac{RPM}{60} \times \left(1 + \frac{B_d}{P_d}\cos\beta\right) \quad (2)$$

$$BSF\ (Hz) = \frac{P_d}{B_d} \times \frac{RPM}{60} \times \left[1 - \left(\frac{B_d}{P_d}\cos\beta\right)^2\right] \quad (3)$$

Approximate ratios between the bearing frequencies and the shaft speed frequency for both types of bearings are shown in Table 2. These ratios correspond to the approximate number of rolling elements coming into contact at the same location on the bearing raceways and the numbers of times a rolling element rotates in every complete shaft revolution. These ratios are useful to determine the number of impacts occurred in one complete shaft rotation and also to calculate the interval between two adjacent impacts.

Table 2: Approximate ratio of bearing frequencies to shaft speed frequency

	Ball Bearing	*Roller Bearing*
BPFO	*3.1*	*4.0*
BPFI	*4.9*	*6.0*
BSF	*2.0*	*2.5*

EXPERIMENTAL SETUP

Test rig setup

The test rig used for this project is the Bently Nevada RK 4 Rotor Kit (Figure 2), which closely simulates the actual rotating machine behaviour. Its unique geometry and its ability for users to isolate and control individual machine characteristics, make it useful as a laboratory tool for theoretical research. The test rig setup consists of a mechanical base, which includes a motor and coupling, rotor shaft, two journal bearings and bearing blocks, a bearing housing and a test bearing, four proximity probes, a probe mount, and a safety cover. A direct current motor speed control device provides power to the rotor kit for controlling the motor speed and also to the Proximitor® assembly. Proximitor® assembly contains five Proximitor® units for proximity probes attachment.

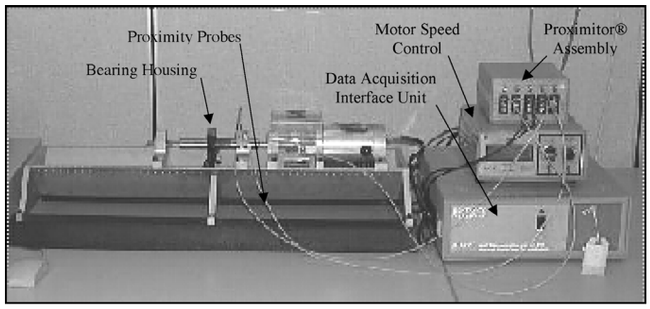

Figure 2: Test rig setup for relative shaft displacement measurement

The test rig is a precision model of a high-speed rotating machine that may be assembled and operated in various configurations. It has a V-frame design that has been developed to provide better control of the housing dynamic stiffness properties. The mechanical tolerances have also been tightened, resulting in more accurate machine behaviour modelling. The RK 4 Rotor Kit motor can closely hold the desired speed with changes in loading conditions. This has been accomplished by incorporating a direct current motor and high performance control circuitry. The motor can run in either a clockwise or counter-clockwise direction and has adjustable slow roll speed capability. In this research, the motor was set to counter-clockwise direction with its rotational speed fixed at 2000 rpm, which is set by using the motor speed control.

A total of four proximity probes were used, where two probes are for relative shaft displacement measurements. The other two probes for Keyphasor® (one-per-turn) phase reference pulse generation and for Motor Speed Control speed sensing. These probes are designed for Bently Nevada RK 4 Rotor Kit Proximitor Assembly, which comes with the rotor kit. The probes were locked in place by tightening the locknut and are set to avoid any contact that could occur between the probe tip and any part of the rotating assembly during extreme vibration conditions as the probes may be mechanically damaged. Two mutually perpendicular proximity probes for measuring the relative shaft displacement are mounted at ±45º from true vertical and oriented in two planes perpendicular to the shaft to avoid adverse electrical coupling, as illustrated in Figure 3. If the probes are installed at an angle of 45º from each other, it could cause cross-talk problems and may lead to misinterpretation of the results. Probes observing the shaft have 0.8 mm gap between the probe tips and the shaft, whereas Keyphasor® and speed control probes have a 0.4 mm gap from the probe tip to the coupling. The gaps for the Keyphasor® and speed control probes is smaller for a larger negative voltage because the coupling is made out of aluminium. Keyphasor® probe is gapped with the notch or keyway 180 degrees away from the probe and the speed control probe is gapped while centred on a tooth. A feeler gauge was used in order to set the gaps correctly. The Keyphasor® probe produces a voltage pulse for each turn of the shaft, called the Keyphasor® signal. This signal was used primarily to measure shaft rotational speed and serves as a reference for measuring vibration phase lag angle.

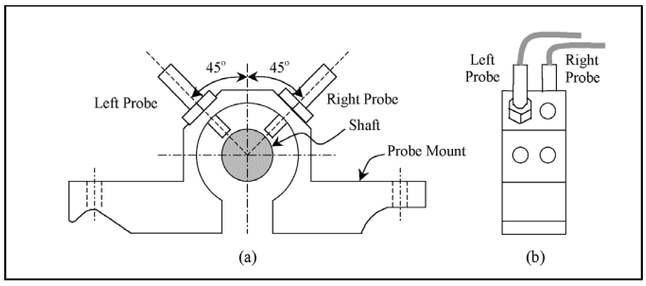

Figure 3 : Schematic diagram of the proximity probes mounted on probe mount, (a) viewed from the drive and (b) viewed from the left side

Data analysis software

The data analysis software was ADRE® (Automated Diagnostics for Rotating Equipment) for WindowsTM software version 3.4 that linked together with a 208-P Data Acquisition Interface Unit (DAIU) were used in this experimental setup. Unlike other general-purpose computer based data acquisition systems, ADRE® for WindowsTM software is specifically designed for capturing machinery data. This system is extremely versatile, incorporating the features and capabilities of oscilloscopes, spectrum analysers, filters, and recording instruments. The 208-P DAIU is a processing unit that interfaces directly to a computer. Two proximity probes for relative shaft displacement measurements and a Keyphasor® probe are connected to the 208-P DAIU inputs through a Proximitor® assembly (Figure 2).

Time waveform analysis

Time waveform analysis can be used effectively for the indication of true amplitude in situation where impacts occur, such as rolling element bearings fault [21]. Inspection of the time waveform can sometimes reveal more information about the signal that the spectrum of the signal does not show. In machine vibration, mechanical impacting like rolling element bearings fault usually causes spikes. For instance a sharp spike and a randomly varying continuous signal can have spectra that look almost identical, while their waveforms are completely different. Thus, once the data acquisition process has been completed, the captured data is analysed with time

waveform analysis. Time waveform plots were plotted to display the instantaneous amplitude of a signal as a function of time. This plot shows the dynamic vibration amplitude of a shaft as observed from the associated proximity probe.

RESULTS AND DISCUSSION

Non-defective bearings

The results for a non-defective ball and roller bearings exhibit a smooth time waveform plots, as shown in Figure 4 and Figure 5, respectively. Both figures also show a slight fluctuation due to tolerances and undulations of the rolling element. As the contact surface between a roller and the raceways is greater compared to a ball, the fluctuations on the roller bearing time waveform curve are more obvious. The Keyphasor® marks on the curves represent the centerline location of the shaft in its path of travel when the keyway is in front of the Keyphasor® probe. Two adjacent Keyphasor® marks (•) corresponds to one complete shaft revolution. A total of six complete shaft revolutions observed from the right probe were shown in the figures. Each of a complete shaft revolution has an interval of 30 milliseconds (33.33 Hz), which is equivalence to the shaft speed frequency at 2000 rpm. A slight change of Keyphasor® marks location in the time wave curve could be due to the sliding motion between the rolling elements and the raceways, as a result of the clearance [22].

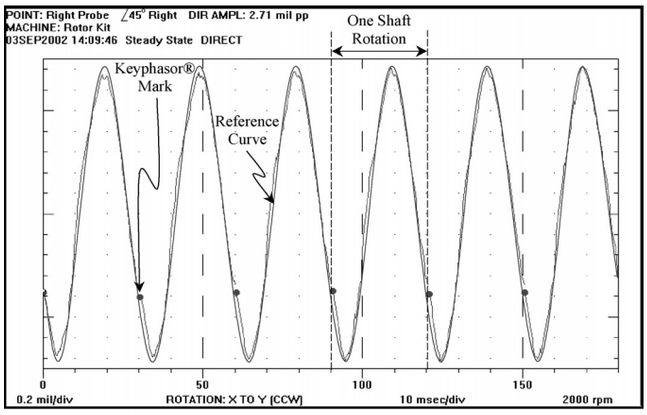

Figure 4: Non-defective ball bearing

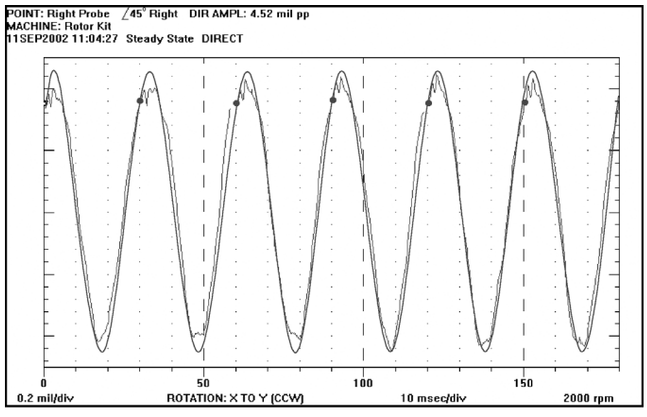

Figure 5: Non-defective roller bearing

Bearings with a single outer race fault

For a single outer race fault, the rolling elements will come into contact with the fault on the bearing outer race. The fault does not move against the proximity probes as the bearing outer ring was fixed onto the bearing housing. As calculated in Table 2 previously, the expected numbers of rolling elements coming into contact with the outer race fault are approximately 3.1 balls and 4.0 rollers, respectively for every complete shaft rotations. From the results presented in Figure 6 to Figure 9, ball and roller bearings with a single outer race fault produced a pronounced spiking time waveform plots. The numbers of spikes that appeared in the time waveform curve for each complete shaft rotation showed that it is equivalent to the numbers of rolling elements coming into contact with the outer race fault. In Figure 6 and Figure 8, a total of three pronounced spikes were seen for every complete shaft rotations with an approximate time period of 9.67 ms between two adjacent spikes. Whereas four pronounced spikes appeared in Figure 7 and Figure 9 with an approximate time interval of 7.50 ms. Due to the sliding motion between the rolling elements and the raceways, the time interval within two adjacent spikes varies less than 3% from the calculated values.

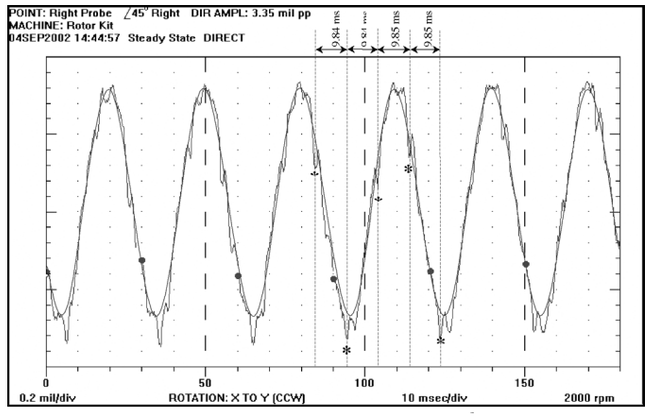

Figure 6: Ball bearing with a single outer race fault located at 0º from the right probe

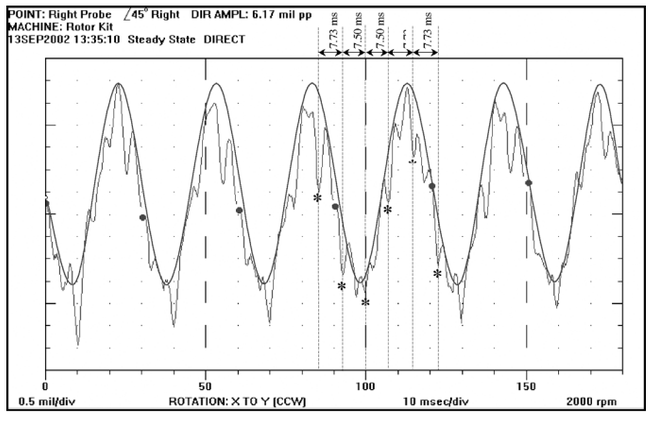

Figure 7: Roller bearing with a single outer race fault located at 0º from the right probe

It was found that the spike direction, either positive or negative, varies with the outer race fault location relative to the probe tip. If the outer race fault is located at 0˚ or in phase with the probe tip, negative spikes were detected in the time waveform curve as marked '*' in Figure 6 and Figure 7. When the balls or rollers come into contact with the "bump" on the

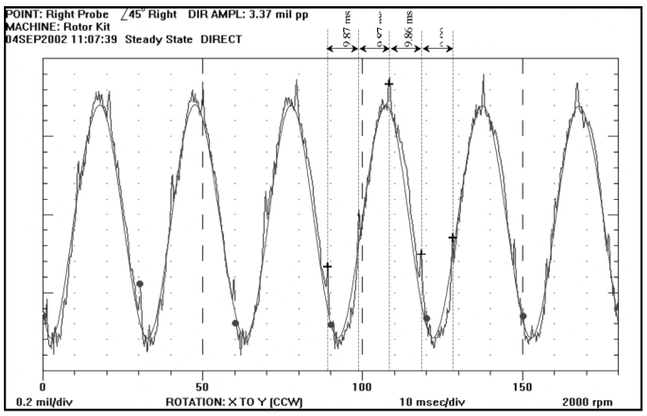

Figure 8: Ball bearing with a single outer race fault located at 180° from the right probe

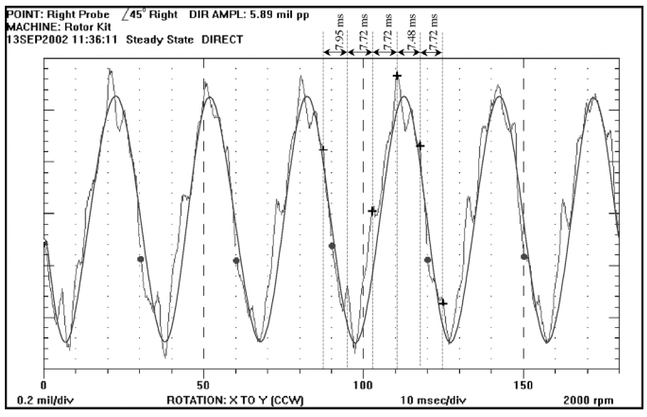

Figure 9: Roller bearing with a single outer race fault located at 180° from the right probe

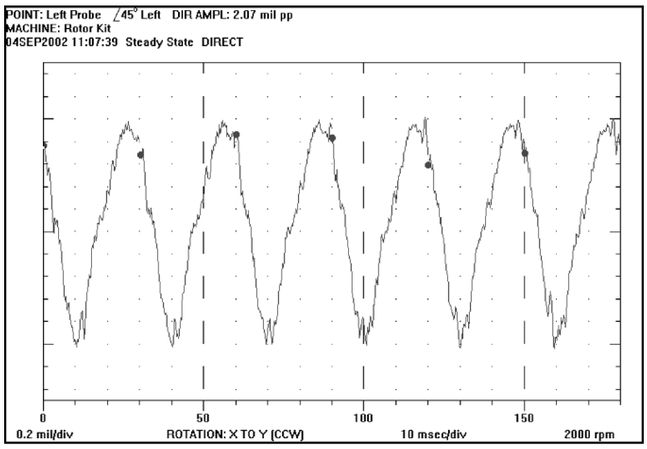

Figure 10: Ball bearing with a single outer race fault located at 90o relative to the left probe

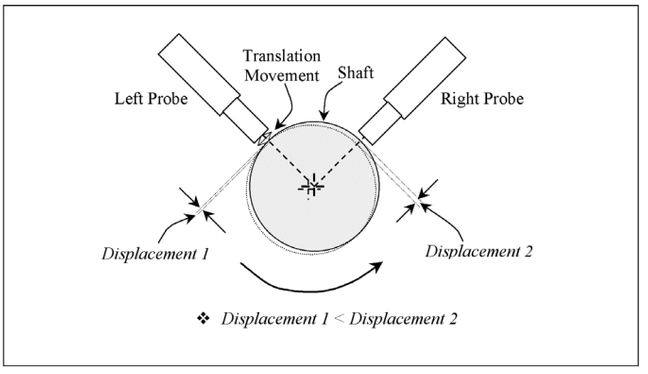

Figure 11: Schematic diagram of a single outer race fault located at 90° from the left probe

bearing outer raceway, produces a location of decreased clearance. Thus, the rolling element to raceways contact at the fault location is actually loaded temporarily over a very short time period [18]. This loading makes the shaft springs away from the probe, resulting in sudden increased in clearance between the probe tip and the shaft surface. Therefore, negative spikes were produced in the time waveform curve. Whereas positive spikes were detected when the outer race fault located at 180° relative to the probe tip, as marked '+' in Figure 8 and Figure 9. In this instance, the rolling element come into contact with the outer race fault and temporarily loading occurs, which springs the shaft towards the probe. Consequently, the clearance between the probe tip and the shaft surface decreases resulting in positive spikes.

In addition, Figure 10 shows the time waveform plot from the left probe when the outer race fault was located at 180° relative to the right probe, where the response was shown in Figure 8. The left probe response only shows slight fluctuations occurring in its time waveform plot without any obvious positive or negative spikes. Similar result was also observed when the outer race fault located in phase relative to the right probe. Such a phenomenon occurs when a single outer race fault is located at 90° from the left probe (as illustrated in Figure 11) will only move the shaft in translation direction relative to the probe tip. Therefore, only a slight displacement was detected as random fluctuations on time waveform curve due to the translation movement of the shaft convex surface near the probe tip.

From this experiment, it was found that the spike magnitude and direction varies with the outer race fault location. If the outer race fault is located at an angle less than 90° (right and left), negative spikes will be detected on the time waveform plot with its highest magnitude when the fault is in phase relative to the probe tip. Whereas if the fault is located at an angle more than 90°, positive spikes will be detected with its highest magnitude when the fault is 180° relative to the probe tip.

Bearing with a single inner race fault

If a fault occurs on the inner race of a bearing, it will come into contact with the rolling elements when the inner ring rotates. Thus, the inner race fault location changes according to the shaft position relative to the probe tip during each shaft rotation. As calculated in Table 2, approximately five balls and six rollers would come into contact with the inner race fault for every complete shaft rotations. Hence, two adjacent spikes are expected to have time intervals of 6.12 ms and 5.00 ms for both types of bearings. As shown in Figure 11 and Figure 12, the time intervals between two adjacent spikes gained from the experiment were very close to the calculated values. It is found that the bearings with an inner race fault indicated a few consecutive positive and negative spikes within one shaft

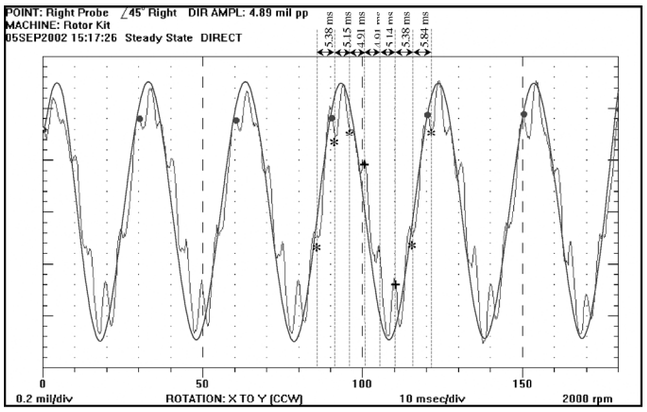

Figure 12: Roller bearing with a single inner race fault

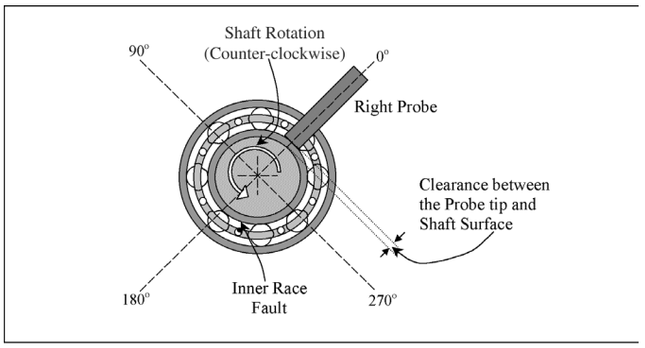

Figure 13: Schematic diagram of a single inner race fault relative to the probe tip

rotation. Such a phenomenon occurs due to the changes of inner race fault location relative to the probe tip, as illustrated in Figure 13.

Based on Figure 13, when the inner race fault rotates within 90º to 270º in counter-clockwise direction relative to the probe tip, it will come into contact with a few rolling elements. Consequently, a few consecutive positive spikes were formed depend on the rolling element bearing geometry. Whereas a few consecutive negative spikes were formed when the fault rotates along 270º to 90º relative to the probe tip. If the inner race fault comes into contact with the rolling element perpendicular to the probe tip, formation of the spike is not obvious as marked 'x' in Figure 11. Only a slight fluctuation was detected due to the translation movement of the shaft convex surface near the probe tip.

Bearings with a single rolling element fault

As shown in Table 2, a single fault on the roller surface is expected to come into contact with a raceway 2.5 times during each shaft rotation. However, for the fault occurring on the rolling element, it will come into contact with both the outer and inner raceways [11]. Thus, the numbers of events for a fault to come into contact with both raceways are (2.5x2) = 5.0 in every shaft rotations. Hence, two adjacent spikes are expected to have an interval of 6.0 ms. Referring to Tables 1 and 2, the tested roller bearing consists of ten rollers and four rollers are expected to come into contact with outer race on the same location for every complete shaft rotation. Therefore, the numbers of shaft rotation for a roller rolled back to its origin is equal to 2.5 rotations. This means there will be an approximately 12.5 positive and negative spikes in every 2.5 times of shaft rotations on the time waveform plot. As presented in Figure 14, a series of several consecutive positive spikes (+) intermittently with a series of several consecutive negative spikes (*) were identified. The numbers of spikes that occur is equivalent to the calculated value (approximately 12 spikes) when a fault on the rolling element rolled back to its origin.

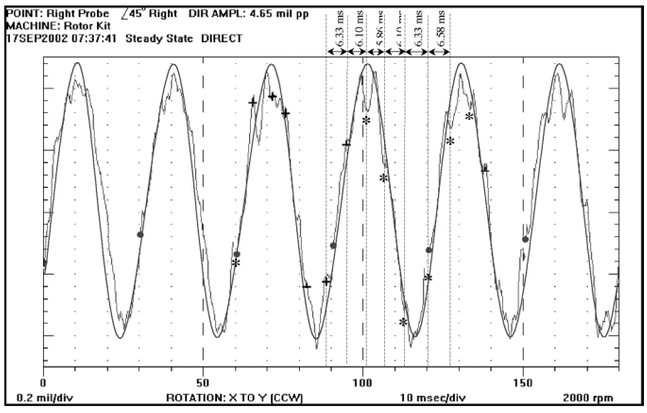

Figure 14: Roller bearing with a single rolling element fault

CONCLUSIONS

Outer race and inner race fault, as well as rolling element fault, which often occur sequentially, can be successfully detected by directly measuring the relative shaft displacement with proximity probes. The fault signal is clearly present with positive or negative spikes, or both in the time waveform curve depending on the types of fault that occurs and its location relative to the probe tip. Spike amplitudes due to faults vary with load and also its location relative to the probe tip. For a fault where metal is removed from the raceway or rolling element surface, i.e., a "valley" instead of a "bump", spike directions would be opposite to those discussed above [18]. This fault produces a location of increased clearance, where the contact between the rolling element and the raceways at the fault is actually unloaded temporarily over a short time period. Consequently, the shaft springs away or towards the probe tip and results in a short duration spike in the time waveform curve. From the experimental data gained in this study, the following general conclusions can be drawn:

1. For a non-defective ball and roller bearings, a smooth time waveform plot without any obvious spikes is observed. Due to the larger contact surface between a roller and the raceways compared to a ball, the fluctuations on the roller bearing time waveform curve are more obvious.
2. For a single outer race fault, spikes occur at the rate of rolling elements coming into contact with the fault and repeat in every complete shaft rotations. The spike amplitude and direction (positive or negative) vary with the fault location relative to the probe tip. In addition, having two mutually perpendicular proximity probes are helpful to determine the fault location.

3. For a single inner race fault, several consecutive positive and negative spikes are seen in every complete shaft rotations due to the changes of fault location relative to the probe tip. The number of spikes (both positive and negative) detected within a single shaft rotation are equal to the number of rolling elements contact with the fault.
4. For a single rolling element fault, spikes occur with an interval related to each time the fault contacts either the outer race or the inner race. Due to the changes of fault orientation and location while the rolling element rolled back to its origin, a series of several consecutive positive and negative spikes are detected intermittently within a few shaft rotations.

REFERENCES

[1] I. Antoniadis, and G. Glossiotis, "Cyclostationary Analysis of Rolling Element Bearing Vibration Signals", *Journal of Sound and Vibration*, Vol. 248, No. 5, pp. 829 – 845, 2001.

[2] R. L. Mott, *Machine Elements in Mechanical Design. 3rd ed.*, New Jersey: Prentice Hall, pp. 535 – 544, 1999.

[3] H. A. Rothbart, *Mechanical Design Handbook*, New York: McGraw-Hill Book Company, Inc., Sections 18 – 19, 1996.

[4] J. Pineyro, A. Klempnow, and V. Lescano, "Effectiveness of New Spectral Tools in the Anomaly Detection of Rolling Element Bearings", *Journal of Alloys and Compounds*, Vol. 310, pp. 276 – 279, 2000.

[5] J. R. Stack, T. G. Habetler and R. G. Harley, "Effects of Machine Speed on the Development and Detection of Rolling Element Bearing Faults", *IEEE Power Electronics Letters*, Vol. 1, No. 1, pp. 19 – 21, 2003.

[6] S. A. McInerny and Y. Dai, "Basic Vibration Signal Processing for Bearing Fault Detection", *IEEE Transactions on Education*, Vol. 46 (1), pp. 149 – 156, 2003.

[7] S. D. Roach, "Designing and Building an Eddy Current Position Sensor", *Sensors*, Vol. 15, No. 9, 1998.

[8] R. Barron, *Engineering Condition Monitoring - Practice, Methods and Applications*, New York: Addison Wesley Longman Inc., 1996.

[9] P. D. McFadden and J. D. Smith, "Model for the Vibration Produced by a Single Point Defect in a Rolling Element Bearing", *Journal of Sound and Vibration*, Vol. 96, No. 1, pp. 69 – 82, 1984.

[10] Y. T. Su and S. J. Lin, "On Initial Fault Detection of a Tapered Roller Bearing – Frequency Domain Analysis", *Journal of Sound and Vibration*. Vol. 155, No. 1, pp. 75 – 84, 1992.

[11] L. Bo, Y. C. Mo, Y. Tipsuwan and J. C. Hung, "Neural-Network-Based Motor Rolling Bearing Fault Diagnosis", *IEEE Transactions on Industrial Electronics*, Vol. 47, No. 5, pp. 1060 – 1069, 2000.

[12] N. Tandon and A. Choudhury, "An Analytical Model for the Prediction of the Vibration Response of Rolling Element Bearings due to a Localized Defect", *Journal of Sound and Vibration*, Vol. 205, No. 3, pp. 164 – 181, 1997.

[13] H. Ohta and N. Sugimoto, "Vibration Characteristics of Tapered Roller Bearings", *Journal of Sound and Vibration*. Vol. 190, No. 2, pp. 137 – 147, 1996.

[14] D. Gluzman, "Recognizing Impending Bearing Failure", *RELIABILITY® Magazine*, pp. 41 – 47, 2001.

[15] B. Yazici, G. B. Kliman, W. J. Premerlani, R. A. Koegl, G. B. Robinson and A. Abdel-Malek, "An Adaptive, On-Line, Statistical Method for Bearing Fault Detection using Stator Current", in *IEEE-IAS Annual Meeting Conference*, Vol. 1, pp. 213 – 220, 1997.

[16] D. E. Bently, "Monitoring Rolling Element Bearings", *ORBIT*, Vol. 3, No. 3, pp. 2 – 4, 1982.

[17] R. Bosman, "REBAM® - Getting Past the Limitations of Seismic Transducers to a More Thorough Root Cause Analysis of a Rolling Element Bearing Failure", *ORBIT*, Vol. 20, No. 1, pp. 7 – 10, 1999.

[18] D. E. Bently, P. Goldman and J. J. Yu, "Rolling Element Bearing Defect Detection and Diagnostics Using REBAM® Probes", *ORBIT*, Vol. 22, No. 2, pp. 12 – 25, 2001.

[19] B. Jones, "Vibrations Help Find Faulty Components", *Evolution 3/99*, pp. 1 – 4, 1999.

[20] Bently Nevada, "Methodology for Monitoring Rolling Element Bearing Machines", *ORBIT*, Vol. 17, No. 3, pp. 18 – 22, 1996.

[21] T. Dunton, "Time Waveform Analysis", *Enteract Papers*, 1998.

[22] M. Tiwari and K. Gupta, "Effect of Radial Internal Clearance of a Ball Bearing on the Dynamics of a Balanced Horizontal Rotor", *Journal of Sound and Vibration*, Vol. 238, No. 5, pp. 723 – 756, 2000.